

University of Texas Rio Grande Valley

ScholarWorks @ UTRGV

Chemistry Faculty Publications and
Presentations

College of Sciences

7-11-2023

Confirmation of N-Hexane as An Inert Co-Solvent in The Production of Functionalized Silicon Nanoparticles from Reactive High-Energy Ball Milling

Julie P. Vanegas

Amanda Reusch

Mark J. Fink

Brian S. Mitchell

Follow this and additional works at: https://scholarworks.utrgv.edu/chem_fac



Part of the [Chemistry Commons](#)

Confirmation of n-Hexane as an Inert Co-Solvent in the Production of Functionalized Silicon Nanoparticles from Reactive High-Energy Ball Milling

Julie P. Vanegas^{3*}, Amanda Reusch¹, Mark J. Fink², and Brian S. Mitchell¹

¹Department of Chemical and Biomolecular Engineering, Tulane University. ² Department of Chemistry, Tulane University. ³ Department of Chemistry, University of Texas Rio Grande Valley Science Building.

Abstract. Alkanes such as n-hexane have been used as co-solvents in the production of functionalized semiconductor nanoparticles from alkenes and alkynes using Reactive High Energy Ball Milling (RHEBM) under the assumption that they are non-reactive under typical milling conditions. In this paper, we report on a comparative study with two hydrocarbon solvents of comparable chain length, 1-hexyne, and n-hexane, and their milling products using three different commercially available silicon precursors, namely single crystal silicon wafers and polycrystalline particles having a nominal size of 4 μm and 1 mm. We found that nanoparticle formation and surface functionalization in all the three silicon systems occurs only with 1-hexyne; n-hexane is non-reactive and does not lead to appreciable functionalized nanoparticle formation under the conditions studied. Nanoparticles (where formed) and microparticle byproducts of appropriate samples were characterized by TEM, FTIR, PL, $^1\text{H}/^{13}\text{C}$ NMR and TGA to separately confirm nanoparticle formation and surface functionalization.

Keywords: Silicon nanoparticles, saturated hydrocarbons, unsaturated hydrocarbons, 1-hexyne, n-hexane

Introduction

Reactive High Energy Ball Milling (RHEBM) is a specialized type of mechanochemical processing in which a solid surface can be functionalized by a reactive liquid in the milling process. Through the combination of particle size reduction (comminution) and surface functionalization, passivated nanoparticles can be formed which are soluble in the surrounding reactive liquid and easily separated from larger, less functionalized material. This procedure has been demonstrated using several solid-liquid combinations, but the most reported systems involve the reaction of silicon surfaces with short-chain alkenes and alkynes¹. A co-solvent – presumed to be inert – is sometimes used along with the reactive ligand to provide sufficient liquid volume in the milling vial when it is prohibitive to use pure ligand (e.g., cost), to serve as a heat transfer medium to the vial walls for highly exothermic reactions, or to stabilize silicon nanoparticles against further oxidation². Inert co-solvents have also been used in the formation of passivated silicon nanoparticles (SiNPs) using other techniques, such as in the thermal decomposition of diphenylsilane in mixtures of octanol and hexane under supercritical conditions³. In either case, it is desirable – though certainly not required – that the inert co-solvent be of comparable chain length to the reactive ligand to maximize nanoparticle solubility, for example, an equimolar mixture of 1-hexyne and n-hexane where the former is the reactive ligand and the latter the inert co-solvent. To date, there have been no studies confirming the non-reactivity of these alkane co-solvents in the RHEBM environment. The energy input to these systems can be large – on the order of 1 W/g,⁴ and temperatures can increase during the milling operation if heat transfer is not properly controlled, so co-solvent inertness should not be assumed.

Herein we report on the comparison of reactivity and reaction products between two representative hydrocarbons, 1-hexyne and n-hexane, on SiNPs formed during RHEBM. Three different silicon sources are

This article has been accepted for publication and undergone full peer review but has not been through the copyediting, typesetting, pagination and proofreading process, which may lead to differences between this version and the [Version of Record](#). Please cite this article as [doi: 10.1002/ppsc.202300052](https://doi.org/10.1002/ppsc.202300052).

This article is protected by copyright. All rights reserved.

used to investigate differences in reactivity: ground silicon wafer and commercially available silicon particles with nominal sizes of 4 μ m and 1mm. Characterization techniques were selected that confirm nanoparticle formation and/or surface functionalization for the two target organic compounds.

Materials and Methods

The silicon starting materials were subjected to Reactive High Energy Ball Milling in organic liquids as previously described.⁵ Characterization of surface bonding include X-Ray Photoelectron Spectroscopy (XPS), liquid phase Nuclear Magnetic Resonance (NMR) spectrometry, Fourier Transform Infrared (FTIR) spectroscopy, and Thermogravimetric Analysis (TGA).

Materials Three different silicon starting materials were utilized: Single crystal silicon wafer (Sigma-Aldrich, single side polished, undoped, mirror finished, 111 orientation, 3 in. diameter \times 0.5 mm thick, undoped, 99.00% purity, 3-4 microhm-cm electrical resistivity @ 0 $^{\circ}$ C). Two commercial scale ground photovoltaic/ semiconductor-grade silicon wafer particulate materials with nominal sizes of 1mm and 4 μ m were also used (GlobeSil, Lexington, KY). Both commercial silicon particulates come from ingot processing and are undoped with at least 99.9999% purity.

Reagent grade 1-hexyne (Sigma-Aldrich, 99%, density 0.715 g/ml) and n-hexane (Sigma-Aldrich, 95%, density 0.678 g/ml) were purified by simple distillation upon receipt. NMR solvent dichloromethane- d_2 , 99.5 atom% (CD_2Cl_2 ; 99.96%) was obtained from Sigma-Aldrich (99 atom % D). Hydrocarbons were distilled under nitrogen and stored over 3 Å molecular sieves and placed in a nitrogen-filled glove box.

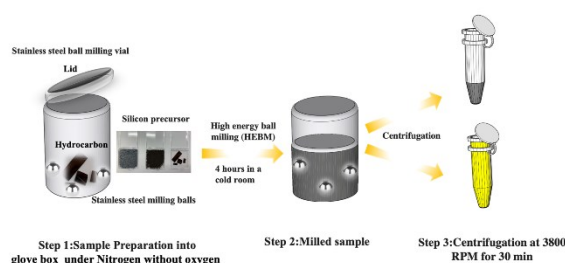


Fig. 1 Silicon particles hydrocarbons-passivated synthesis (SiPs@hydrocarbons) by RHEBM. Schematic diagram of the silicon particles with hydrocarbon synthesis. (SiPs@hydrocarbons) under nitrogen. Silicon precursor (5g) and hydrocarbon (22.0 g total) (1:4 %m/m) were added into a hardened stainless steel ball milling vial with three hardened stainless steel milling balls (1.2cm in diameter, 8.1g each) in a nitrogen filled glove box.

Surface Reactions in RHEBM. Silicon precursor (5g) and hydrocarbon (22.0 g total) were added to a hardened stainless steel milling vial along with three hardened stainless steel milling balls (1.2cm in diameter, 8.1g each) in a nitrogen filled glove box. The silicon wafer chunks varied in size and shape, with dimensions ranging from just under 1.0 cm to just over 1.5 cm. The commercial-grade silicon particulate sizes were as previously stated (4 μ m and 1mm). It is recommended that the loading of the vial does not exceed approximately 50% of the

available volume⁶; the reagent-grade organic liquid is added to the vial by weight so its volume varies from 20-25 mL depending on the solvent density.

The contents of the vial were subjected to RHEBM using a SPEX CertiPrep 8000D Mixer/Mill for 4 hours in a cold room. After RHEBM was complete the milled samples were separated into soluble (supernatant) and insoluble (pellet) fractions by centrifugation at 3800 RPM for 30 min (Fig 1). The supernatant was passed through a 200 nm in-line filter, the effluent from which was rotary-evaporated and pumped for 24 hours to remove any excess unreacted hydrocarbon, then weighed. The pellet material was also dried for 24 hours to remove any excess unreacted hydrocarbon, then weighed. The resulting supernatant solid product is labeled silicon nanoparticles (SiNPs) and the resulting pellet solid product is labelled silicon microparticles (SiMPs).

Process Yield for Nanoparticle Formation. Process yield was calculated from a ratio of the weight of SiNPs to the weight of silicon starting material (nominally 5g in each experiment). The contribution of hydrocarbon covalently bound to the surface of the nanoparticles was ignored because surface coverage (assumed to be relatively constant) is not known and because the yield values are only used for relative, comparative purposes.

XPS Spectra for Elemental Analysis. XPS measurements were conducted on a VG Scientific MKII system using a Mg K α anode as excitation source ($h\nu = 1253.4$ eV). The pressure in the chamber during analysis was $<5 \times 10^{-8}$ mbar. The samples were deposited on indium foil via evaporation and were 5 mm square and 4 mm thick. Spectral peak fitting and deconvolution was performed with CasaXPS using Gaussian-Lorentzian line shapes.

FTIR for Bonding Analysis. FTIR spectra were recorded at 1 cm^{-1} resolution with 2000 scans on a Thermo Nicolet Nexus 670 FTIR instrument, enabling easy measurement of the spectra of solids and liquids. For ATR, a few milligrams of SiNPs powder were placed on the optic window with a germanium glass and the compression clamp engaged to 6 psi to ensure good contact between the sample and the crystal.

PL Analysis. Photoluminescence spectra of supernatant solutions were taken with a Varian Cary Eclipse fluorescence spectrophotometer at room temperature in quartz cuvettes with an optical pathlength of 1.00 cm. All emission spectra were recorded with an excitation wavelength of 300 nm. PL data were acquired using a concentration of 3mg/mL for SiNPs@1-hexyne (in methanol). The silicon microparticles milled in n-hexane result in small amounts of particles not suitable for dispersion in methanol.

NMR for Structural Analysis ^1H and ^{13}C NMR spectra were recorded at 300 and 75 MHz, respectively, using a Bruker DSX 300 NMR spectrometer, Deuterated dichloromethane (CD_2Cl_2) was used as a solvent. ^1H and ^{13}C NMR chemical shifts are reported in ppm and are referenced to CD_2Cl_2 signals ($\delta=5.32$ and 53.5 ppm, respectively).

TEM/SEM Images for Morphology. TEM-measurements were collected on a 300 kV FEI Tecnai G2 F30 Transmission Electron Microscope. SEM photomicrographs were acquired on a Hitachi 4800 High-resolution SEM, 1.0 nm resolution at 15kV. SiNPs samples were deposited on carbon films 48h prior to measurement in

This article is protected by copyright. All rights reserved.

each of the means of dispersion and dried in a vacuum. The size distribution of the nanoparticles was determined by ImageJ software⁷ based on TEM images. Statistical analysis was obtained by measuring the diameters of 200 nanoparticles.

TGA Analysis. A TA Instruments TGA Q500 Thermogravimetric Analyzer/Pfeiffer was used in the temperature range of 25-1000°C with sample heating at the rate of 5° per minute under flowing nitrogen.

Results and Discussion

The milling of silicon in both dry and wet environments is well studied^{8,9}. In fact, it has received renewed interest as silicon and silicon-based alloys and nanocomposites are strong candidates for anode materials in lithium-ion batteries¹⁰. A recent review of both wet and dry milling of silicon for this application highlights the advances and challenges¹¹. Such milling parameters as milling time, ball/powder ratio, and milling media size have been studied for silicon in these non-reactive systems and showed that the d_{90} particle diameter of 12 μm did not change significantly from 4 to 8 hours of milling time in 20 mm grinding beads¹².

However, in the potentially reactive wet milling environments studied here, the evolution of nanoparticles follows a different path. Functionalized nanoparticles can be formed early in the milling process where they remain solubilized in the surrounding liquid and do not participate significantly in further size reduction. Traditional ball milling parameters like milling time, ball/powder ratio, and milling media size become less important in determining whether the liquid medium is reactive or not with the milled material.

As a result, nanoparticle formation is the key indicator of surface functionalization in these reactive milling systems⁵, that is, only those particles that are sufficiently small and sufficiently surface functionalized will remain soluble in the reactant liquid mixture during centrifugation. As shown in Table 1, only silicon reacted with 1-hexyne resulted in surface-functionalized nanoparticles that could be recovered from the supernatant after centrifugation and filtration. The yields from all three silicon source materials functionalized with 1-hexyne are consistent with process yields in

Table 1 Silicon Nanoparticles SiNP@1-hexyne Yield %

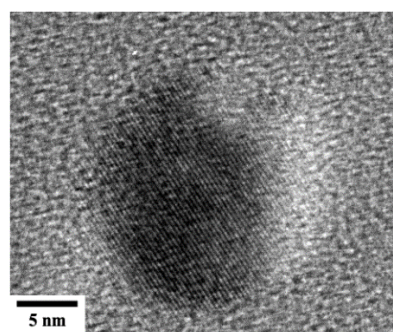
	Wafer	GlobeSil 4 μm	GlobeSil 1mm
1-hexyne	9.4%	11.7%	7.6%

similar RHEBM systems.¹ Though yield could potentially be increased with the adjustment of milling parameters such as time, the four hour milling times here were sufficient to show that functionalized nanoparticles were formed only with 1-hexyne as a reactant liquid. Only impurity levels of solid material were recovered from the supernatant of centrifuged samples from the milling of silicon in n-hexane. This is

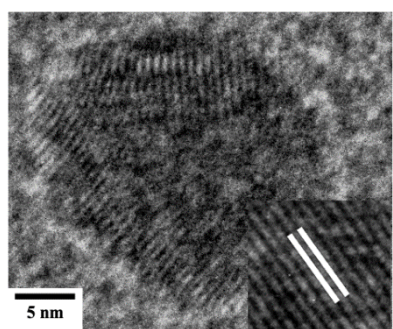
This article is protected by copyright. All rights reserved.

evidence that no significant reaction is occurring with n-hexane under these process conditions. As a result, characterization of SiNPs functionalized with 1-hexyne will first be discussed, followed by characterization of materials obtained from milling in n-hexane.

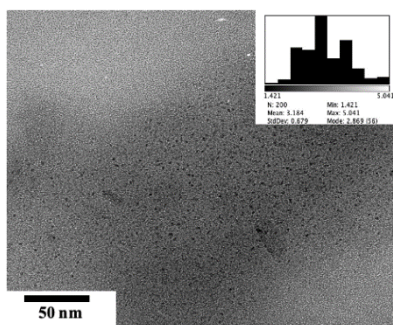
Silicon Milled in 1-Hexyne. The average sizes of nanoparticles formed from the reaction of silicon with 1-hexyne were 4.5 ± 1.6 nm, 3.1 ± 0.67 nm, and 2.1 ± 0.5 nm for the wafer, 4 μ m GlobeSil, and 1mm GlobeSil starting materials, respectively, as determined by TEM histograms (Figure 2, inset). Representative TEM images for the functionalized SiNPs from wafer and polycrystalline powders are shown in Figure 2. The nanoparticles derived from the wafer material show uniform lattice fringes with spacing of 0.080nm indicative of a single crystalline material. On the other hand, nanoparticles from the polycrystalline powder show lattice fringes which intersect along multiple boundaries with an interplanar spacing of 0.45 Å, indicating that the nanoparticles contain numerous single crystalline domains.



a



b



This article is protected by copyright. All rights reserved.

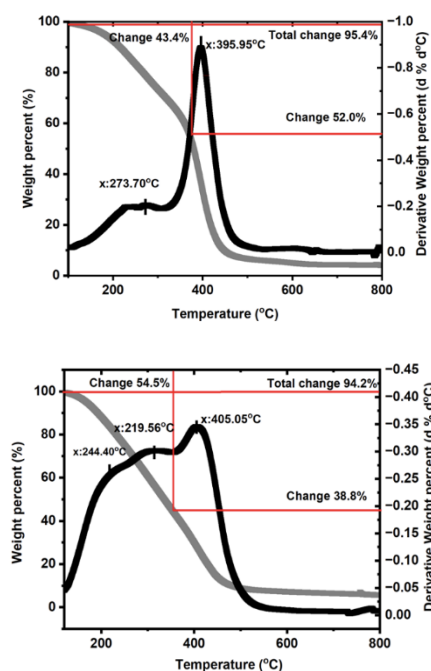
c

Fig.2. TEM images of major sphere shapes and various precursors, well dispersed and polycrystalline. TEM images of Si nanoparticles with scale bars: 5 nm (a from wafer, b from GlobeSil 1mm), 50 nm (c from GlobeSil 4mm)

All three 1-hexyne functionalized SiNPs are also characteristically photoluminescent (not shown) with a well-defined Stokes shift and emission in the 400-500 nm range as previously reported.¹ Since no SiNPs for the n-hexane reactions were obtained, neither TEM nor particle size analyses were performed.

Additional support reaction in the 1-hexyne system comes from TGA, FTIR, and NMR results.

Thermogravimetric analysis of the 1-hexyne functionalized silicon nanoparticles (Figure 3) shows similar overall weight losses in the range of 78-95%, but with different weight loss characteristics. In all samples, weight loss below about 200°C can be attributed to the loss of adsorbed water and residual organic solvent.^{13,14} Wafer produced nanoparticles (top) show two distinct weight losses – the first broad weight loss above 200°C and the second more defined loss centered at 396°C as indicated by the derivative weight loss curve. GlobeSil 4µm-derived nanoparticles (Figure 3 middle) show a similar, but less defined mass loss with derivative peaks at 320°C and 406°C. GlobeSil 1mm-derived nanoparticles, however, show a steady polynomial-like decrease with no distinct mass loss events and a total loss of 78%.



This article is protected by copyright. All rights reserved.

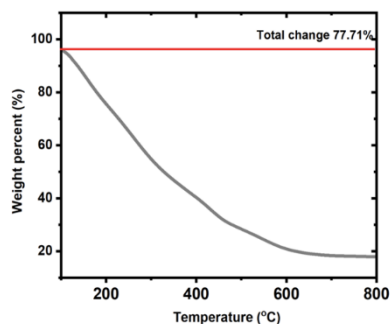


Fig. 3 Percentage (left axis) and derivative (right axis) weight loss curves with temperatures for SiNPs functionalized with 1-hexyne for wafer (top), 4 μ m GlobeSil (middle) and 1mm GlobeSil (bottom) starting materials.

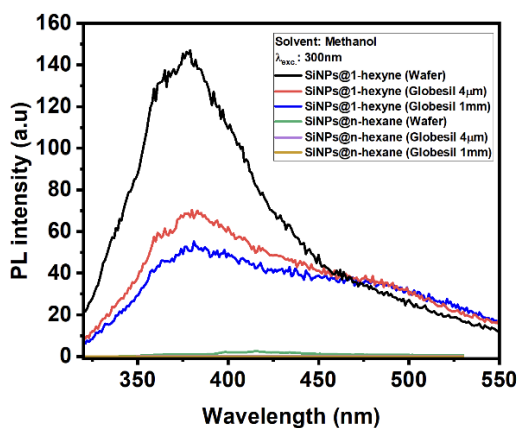


Fig. 4. Emission spectra in methanol of (black, red, and blue) SiNPs@1-hexyne and (green, purple, and yellow) SiNPs@n-hexane. Emission spectra of SiNPs@1-hexyne and SiNPs@n-hexane at = 300 nm, respectively.

Passivation of silicon nanoparticles with organic molecules is known to affect their photoluminescence (PL) properties¹⁵. In the case of 1-hexyne passivation, the resulting silicon nanoparticles exhibit a broad photoluminescence at approximately 374 nm when excited at 300 nm. The intense PL is likely due to the quantum size effects of the silicon nanoparticles or possibly due to surface trap states. On the other hand, when silicon is milled with n-hexane, the PL spectrum shows no significant emission when solutions are excited at 300 nm (Figure 4). This is due to the fact that the silicon microparticles are largely insoluble in methanol.

Figure 4 shows a comparison of the PL spectra of silicon nanoparticles solutions from milling in 1-hexyne and n-hexane, with the former showing a high intensity photoluminescence peak and the latter showing little or no emission.

The existence of a chemisorbed surface layer is further confirmed through FTIR analysis. Characteristic peaks for the terminal triple bond in 1-hexyne are at 2130 cm^{-1} and 2200 cm^{-1} and its associated acetylenic C-H stretching vibration is at 3337 cm^{-1} . A C-H bending vibration also appears at 950 cm^{-1} . The FTIR spectra of the 1-hexyne functionalized nanoparticles (Figure 5) however show none of this characteristic 1-hexyne vibrations but instead show vinylic C-H stretching bands at $2800\text{--}3000\text{ cm}^{-1}$. Evidence of a weak olefinic stretch around $\sim 1686\text{ cm}^{-1}$ is also observed. The pronounced peaks at ~ 1385 and $\sim 1475\text{ cm}^{-1}$ correspond to CH bending vibrations of the alkyl chain and the $\sim 947\text{ cm}^{-1}$ peak corresponds to a Si-C stretching vibration, indicating that the 1-hexyne is indeed bound covalently to the surface of the particle. Weak vibrational bands in the $950\text{--}1079\text{ cm}^{-1}$ region of the spectrum may be attributed to residual Si-O bonds on the surface.

Finally, NMR analysis of the functionalized nanoparticle solutions provides structural evidence of surface functionalization by 1-hexyne (Figure 6). In the ^1H NMR spectrum (Figure 6, top), resonances due to alkyl chain hydrogens (0.88 to 1.26 ppm) are evident as well as vinylic resonances spanning from 6.5 to 8.5 ppm . In the ^{13}C NMR spectrum (Figure 6, bottom) shows four resonances in the olefinic region at 125.9 , 126.8 , 129.4 and 138.4 ppm . Several resonances ($15\text{--}50\text{ ppm}$) appear in the alkyl carbon range of the spectrum. These results are consistent with previous studies of SiNPs functionalized with 1-octyne⁴. In this study, two primary bonding modes of the hydrocarbon with the silicon surface are proposed. The first is through a surface-bound silicon radical formed during milling which reacts via radical addition to alkyne forming a transient vinyl radical. This vinyl radical undergoes hydrogen abstraction with another 1-hexyne molecule in solution resulting in a surface bound alkene. The second structure is the result of [2+2] cycloaddition of the alkyne to silicon dimer surface pairs.^{4,16}

Silicon Milled in n-hexane for the silicon precursors milled in n-hexane, direct comparison of potential reaction products with 1-hexyne is only possible for the microscale products since no nanoscale products were recovered in milling experiments with n-hexane after centrifugation. For these microscale products, NMR analysis was not possible because they were not soluble in any NMR solvent, and TGA analysis was not helpful as less than 1% weight loss was observed in all microscale samples due to the lower surface-to-volume ratio of these larger particles. As a result, the key comparative technique for microscale materials was XPS.

XPS provides the most compelling evidence for a lack of C-H activation in n-hexane milled silicon. As shown in Figure 7, a comparison of XPS results for silicon milled in 1-hexyne (middle spectra for all three silicon sources) with silicon milled in n-hexane (bottom spectra for all three silicon sources) shows the presence of a Si-C environment centered at $100\text{--}101\text{ eV}$ ^[17-19] (green peak) in microscale silicon milled in 1-hexyne that does not exist for microscale products milled in n-hexane. In fact, the n-hexane milled microscale products do not differ substantially from the unmilled silicon precursors (Figure 7, top spectra) where both metallic silicon peaks at $98\text{--}99\text{ eV}$ and a broad Si-O_x silicon suboxide peak at 102 eV are evident.^{20,21}

This article is protected by copyright. All rights reserved.

Conclusions

Silicon nanoparticles (SiNPs) surface functionalized with 1-hexyne in Reactive High Energy Ball Milling (RHEBM) were formed from three different silicon sources. Silicon wafer and commercially available silicon of two different particle sizes (4 μm and 1mm) produced functionalized nanoparticles of nominal size 3 nm when milled in 1-hexyne and were subsequently characterized by spectroscopy and weight loss techniques to provide evidence of functionalization. These same three silicon sources milled with n-hexane, however, did not lead to appreciable nanoscale material indicating lack of surface functionalization in this system. Furthermore, surface characterization of the n-hexane milled silicon microscale products produced insufficient evidence of Si-C bonds as determined by FTIR and XPS to support surface functionalization independent of nanoparticle formation. We thus conclude that n-hexane can be considered an inert co-solvent in RHEBM processes under these conditions.

These findings are limited to the inertness of n-hexane only but have implications to the use of other straight-chain hydrocarbons in RHEBM, especially n-alkanes. Just as we have shown that the formation of functionalized silicon nanoparticles in 1-octyne was extensible to a variety of other alkynes, alkenes, and alkanes with other terminal functional groups¹, the inertness of n-hexane as a co-solvent suggests that other short-chain n-alkanes may be similarly suitable as inert co-solvents. The use of inert co-solvents in RHEBM is important from a cost reduction standpoint as n-alkanes are less expensive than their alkene or alkyne counterparts and the amount of reactive liquid for surface reactions is generally small. In future work the previously assumed non-reactivity of other common co-solvents such as benzene and toluene should be studied.

Associated Content

Supporting Information

The authors confirm that the data supporting the findings of this study are available within the article and its supplementary materials. Moreover, the raw data are available from the corresponding author (JPV) upon reasonable request. These data include physical appearance of the starting materials, synthetic procedure of SiNPs, samples characterization, XPS, and NMR data.

Author Information

Corresponding Author

This article is protected by copyright. All rights reserved.

Julie P. Vanegas. University of Texas Rio Grande Valley. Department of Chemistry. University of Texas Rio Grande Valley. Science Building. 1201 W University Dr, Edinburg, TX 78539 (USA) E-mail: Julie.vanegas@utrgv.edu ORCID #0000-0002-5811-1382

Authors

Amanda Reusch. Tulane University. Department of Chemical and Biomolecular Engineering. 300 Lindy Boggs, New Orleans, LA, 70118 (USA) E-mail: areusch@tulane.edu ORCID #0000-0002-6741-8925

Mark. J. Fink. Tulane University. Department of Chemistry. 2015 Percival Stern Hall. New Orleans, LA, 70118 (USA) E-mail: fink@tulane.edu, ORCID # 0000-0003-4286-6200

Brian S. Mitchell. Tulane University. Department of Chemical and Biomolecular Engineering. 300 Lindy Boggs, New Orleans, LA, 70118 (USA) E-mail: brian@tulane.edu, ORCID # 0000-0002-9037-6364

Conflict of Interest

The authors declare that the research was conducted in the absence of any commercial or financial relationships that could be construed as a potential conflict of interest.

Acknowledgment

The authors wish to thank the Louisiana Board of Regents Industrial Ties Research Subprogram [LEQSF (2018-21)-RD-B-06] for funding this research.

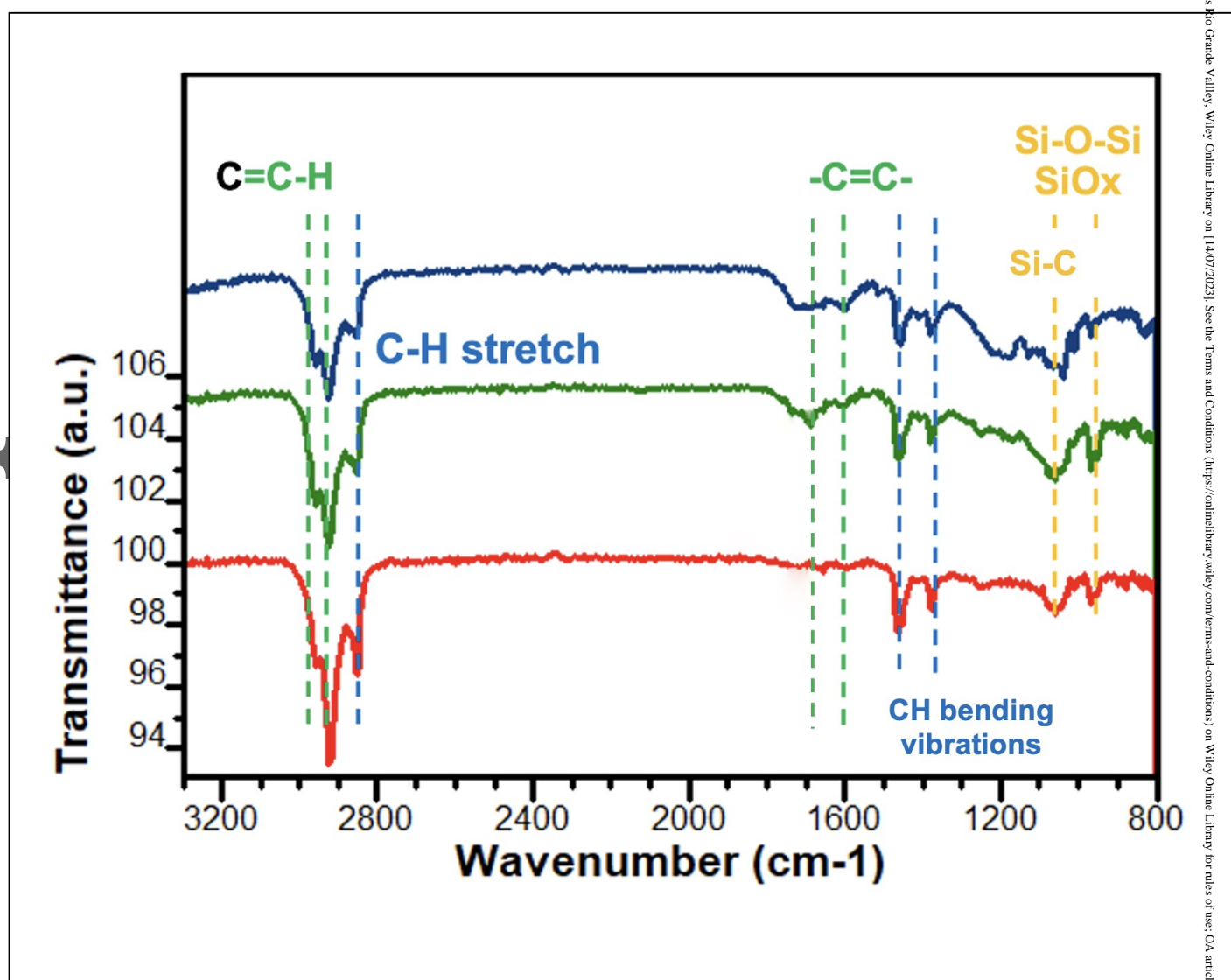
References

- (1) Heintz, A. S., Fink, M. J., Mitchell, B. S. Silicon nanoparticles with chemically tailored surfaces. *Applied Organometallic Chemistry* 2010, 24 (3), 236-240. DOI: 10.1002/aoc.1602.
- (2) Reindl, A., et al. "Dispersing and stabilizing silicon nanoparticles in a low-epsilon medium." *Colloids and Surfaces A: Physicochemical and Engineering Aspects* 320.1-3 (2008): 183-188.
- (3) Holmes J., Ziegler K., Doty R., Pell L., Johnston K., and Korgel B., Highly luminescent silicon nanocrystals with discrete optical transitions. *Journal of the American Chemical Society* 2001, 123(16): 3743-3748. DOI: 10.1021/ja002956f.
- (4) Delogu F.; Mulas G.; Schiffini L.; Cocco G.; Mechanical work and conversion degree in mechanically induced processes. *Materials Science and Engineering: A* 2004 25;382(1-2):280-7.
- (5) Heintz, A. S., Fink, M. J., Mitchell, B. S. Mechanochemical Synthesis of Blue Luminescent Alkyl/Alkenyl-Passivated Silicon Nanoparticles. *Advanced Materials* 2007, 19 (22), 3984-3988. DOI: 10.1002/adma.200602752.
- (6) Suryanarayana, Cury. "Mechanical alloying and milling." *Progress in materials science* 46.1-2 (2001): 1-184.
- (7) Schneider, C. A., Rasband, W. S., Eliceiri, K. W. NIH Image to ImageJ: 25 years of image analysis. *Nature Methods* 2012, 9 (7), 671-675. DOI: 10.1038/nmeth.2089.

This article is protected by copyright. All rights reserved.

- (8) Shen, T., Koch, C., McCormick, T., Nemanich, R., Huang, J., & Huang, J. The structure and property characteristics of amorphous/nanocrystalline silicon produced by ball milling. *Journal of Materials Research* 1995, 10(1), 139-148. doi:10.1557/JMR.1995.0139
- (9) Švrček V., Rehspringer J.L., Gaffet E., Slaoui A., Muller J.C. Unaggregated silicon nanocrystals obtained by ball milling. *Journal of Crystal Growth* 2005, 1;275(3-4):589-97.
- (10) Zheng P., Sun J., Liu H., Wang R., Liu, C., Zhao Y., Li J., Zheng Y., Rui X. Microstructure Engineered Silicon Alloy Anodes for Lithium-Ion Batteries: Advances and Challenges. *Batteries & Supercaps* 2023, 6.1,e202200481.
- (11) Yang H., Lin S., Cheng A., He F., Wang Z., Wu Y., Zhang Y. Recent Advances in Ball-Milling-Based Silicon Anodes for Lithium-Ion Batteries. *Energies* 2023, 16.7,3099.
- (12) Eikeland B. and Kleiv R. Silicon powder properties produced in a planetary ball mill as a function of grinding time, grinding bead size and rotational speed. *Silicon* 2020, 12,2413-2423.
- (13) Ghamarpoor R., Jamshidi M. Synthesis of vinyl-based silica nanoparticles by sol-gel method and their influences on network microstructure and dynamic mechanical properties of nitrile rubber nanocomposites. *Sci Rep* 2022, 12 (1), 15286. DOI: 10.1038/s41598-022-19664-w
- (14) Liu, Z., Huang, J., Zhao, X., Huang, H., Fu, C., Li, Z., Cheng, Y., Niu, C., Zhang, J. A Facile Path to Graphene-Wrapped Polydopamine-Entwined Silicon Nanoparticles with High Electrochemical Performance. *Chempluschem* 2019, 84 (2), 203-209. DOI: 10.1002/cplu.201800554 From NLM PubMed-not-MEDLINE.
- (15) Dasog, M.; De los Reyes, G. B.; Titova, L. V.; Hegmann, F. A.; Veinot, J. G. C. "Size Vs Surface: Tuning the Photoluminescence of Freestanding Silicon Nanocrystals across the Visible Spectrum Via Surface Groups" *ACS Nano* 2014, 8, 9636-9648.
- (16) Tao, F., Xu, G. Q. Attachment Chemistry of Organic Molecules on Si (111)-7 × 7. *Accounts of Chemical Research* 2004, 37 (11), 882-893. DOI: 10.1021/ar0400488. Lin, Y.; Avvacumova, M.; Zhao, R.; Chen, X.; Beard, M. C.; Yan, Y. Triplet Energy Transfer from Lead Halide Perovskite for Highly Selective Photocatalytic 2 + 2 Cycloaddition. *ACS Applied Materials & Interfaces* 2022, 14 (22), 25357-25365. DOI: 10.1021/acsami.2c03411.
- (17) Wang P., Bater, S., Zhang, L., Ascherl, M., Craig Jr, J. XPS investigation of electron beam effects on a trimethylsilane dosed Si (100) surface. *Applied surface science* 1995, 90 (4), 413-417.
- (18) Yamamoto K., Koga, Y., Fujiwara, S. XPS studies of amorphous SiCN thin films prepared by nitrogen ion-assisted pulsed-laser deposition of SiC target. *Diamond and Related Materials* 2001, 10 (9), 1921-1926. DOI: [https://doi.org/10.1016/S0925-9635\(01\)00422-8](https://doi.org/10.1016/S0925-9635(01)00422-8).
- (19) Ibrahim F., Wilson, J. I. B., John, P. Photo-oxidation of a-Si:C:H studied by in situ XPS. *Journal of Non-Crystalline Solids* 1995, 191 (1), 200-204. DOI: [https://doi.org/10.1016/0022-3093\(95\)00312-6](https://doi.org/10.1016/0022-3093(95)00312-6).
- (20) Seah M. P., Spencer, S. J. Ultrathin SiO₂ on Si II. Issues in quantification of the oxide thickness. *Surface and Interface Analysis* 2002, 33 (8), 640-652. DOI: <https://doi.org/10.1002/sia.1433>.

(21) Jensen, D. S., Kanyal S. S., Madaan, N., Vail, M. A., Dadson A. E. Engelhard, M. H.; Linford, M. R. Silicon (100)/SiO₂ by XPS. *Surface Science Spectra* 2013, 20 (1), 36-42. DOI: 10.1116/11.20121101.



This article is protected by copyright. All rights reserved.

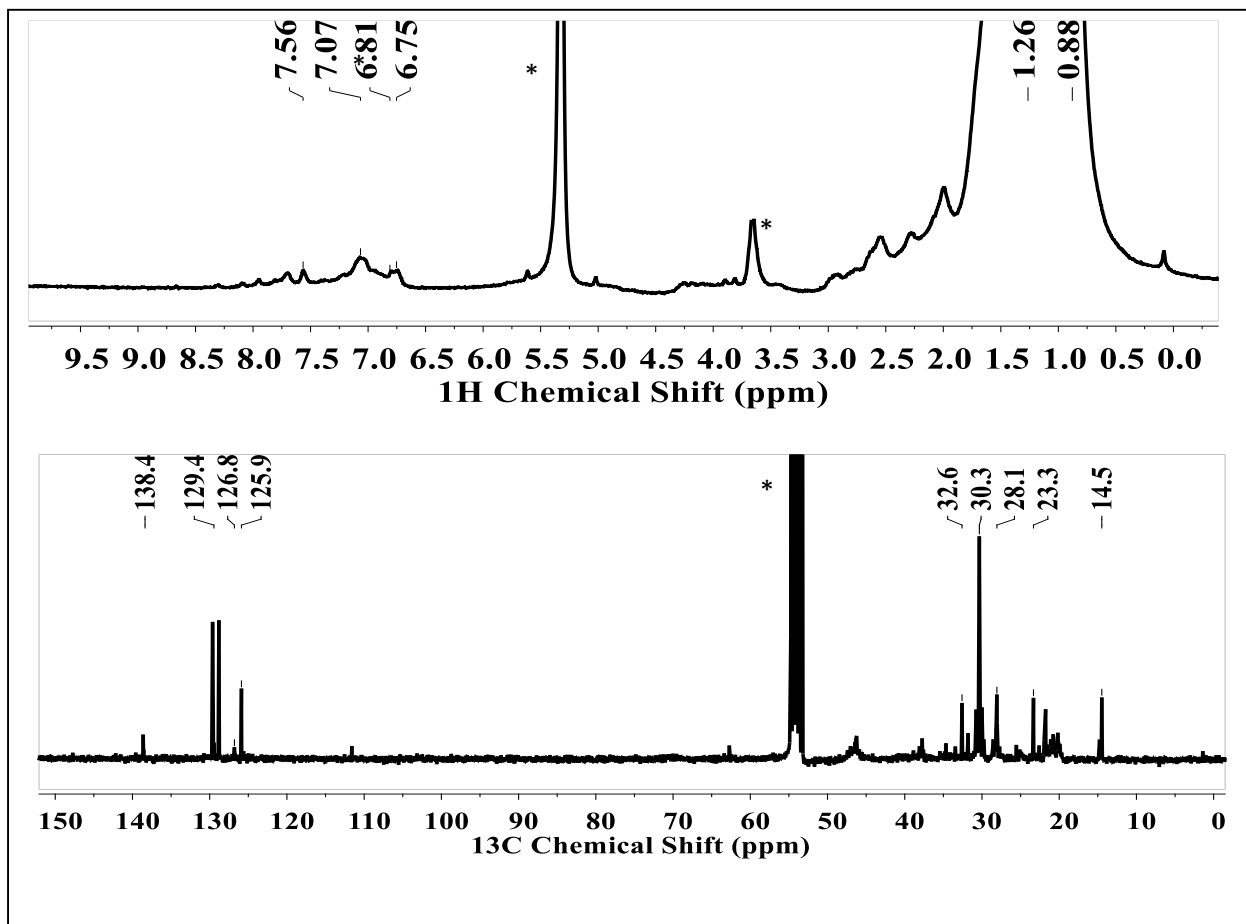
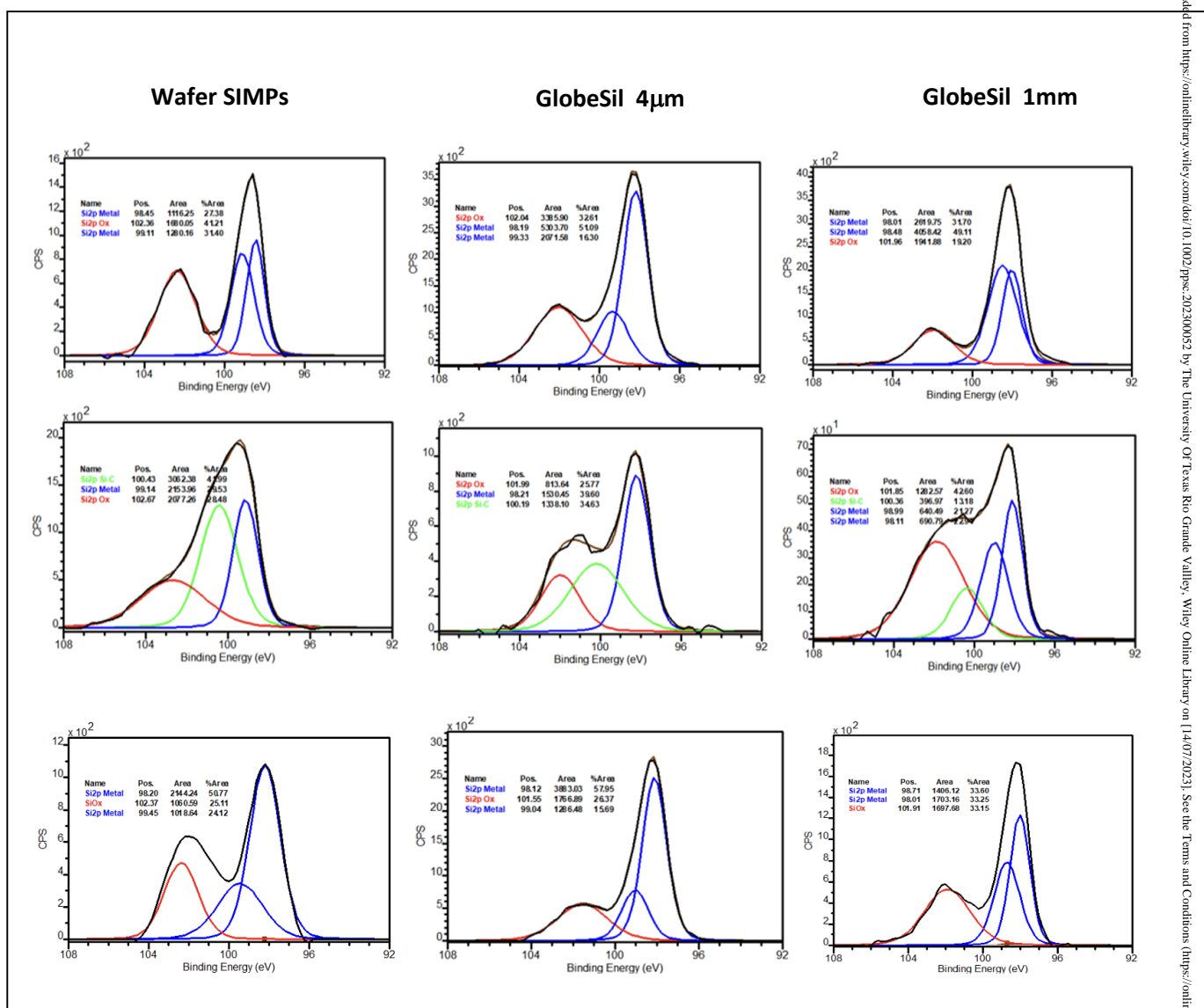


Fig. 6 ¹H NMR (top) and ¹³C NMR spectra of 1-hexyne functionalized SiNPs from wafer. * Residual dichloromethane d-2 and ** milling impurities.



TOC

